PHYSICAL REVIEW E VOLUME 60, NUMBER 2 AUGUST 1999

Trichotomous noise-induced transitions

Romi Mankin and Ain Ainsaar*
Department of Natural Sciences, Tallinn University of Educational Sciences, Narva maantee 25, 10120 Tallinn, Estonia

Eerik Reiter
Institute for Physics, Tallinn Technical University, Ehitajate tee 5, 19086 Tallinn, Estonia

(Received 19 January 1999)

A nonlinear one-dimensional process driven by a multiplicative exponentially correlated three-level Markovian noise (trichotomous noise) is considered. An explicit second-order linear ordinary differential equation for the stationary probability density distribution is obtained for the process. In the case of a linear process with an additive trichotomous noise the exact formula for the steady-state distribution is obtained. The well-known dichotomous noise can be regarded as a special case of the trichotomous noise. As a rule, the system variable has three specific values where the probability density distribution can be singular. For the case of the Hongler model the dependence of the behavior of the stationary probability density on the noise parameters is investigated in detail and illustrated by a phase diagram. Applications to the Gompertz and Verhulst models are also discussed. [S1063-651X(99)03708-3]

PACS number(s): 05.40.−a, 02.50.−r

I. INTRODUCTION

Within the past two decades the behavior of open systems depending on the environment has deserved considerable attention. Simple physical, biological, chemical, and other systems can take several unusual stationary states in case their parameters are affected by a noiselike influence from the environment (for reference surveys see [1–3]). Such an influence can be rather complex, but only a limited number of abstractions admit exact solutions in theory. The most productive abstraction is the case of Gaussian white noise that corresponds to a vanishing correlation time of the noise; this is closely related to diffusion processes in physics.

White noises have some nonphysical properties and their application requires some care (cf. [4]). Thus, in the past decades attention has been paid to colored noises of finite correlation times as more physical ones. Of these, the one most frequently used is the Gaussian colored noise (GCN) generated by the Ornstein-Uhlenbeck process. Unfortunately, it turns out that a rather limited class of noise-driven model systems admits exact solutions in the presence of GCN [2,3].

Another noise popular because of its tractability is symmetric dichotomous noise, also called random telegraph noise [2,5–7]. Kitahara *et al.* [5,6] have calculated exact stationary probability densities for the Verhulst system coupled to dichotomous noise. They have also presented a comprehensive phase diagram to demonstrate the noise-induced transitions in the space of noise parameters. Their success inspired us to seek solutions of a more general case of random three-level telegraph processes that may be called *trichotomous noise* [8].

A three-level Markovian noise different from the trichotomous noise used by us has been applied to investigate the reversals of noise-induced flow [9,10]. It has been shown that the direction of the flow can depend on the correlation time of the noise as well as on the flatness parameter (see also [11]). As to the noise-induced transitions, their dependence on the flatness has hardly been studied at all, for flatness is constant at both the dichotomous noise and GCN, being equal to 1 and 3, respectively.

As dichotomous noise switches a deterministic process randomly between two static perturbation states, the stationary probability density distribution of the system variable remains between two distinct values, taking different extrema for various noise parameter regimes. By configurations of those extrema the phase diagram of the noise parameters is divided into domains. As trichotomous noise takes, in addition, a zero value with a given probability, the support of the probability density has also a third characteristic point that corresponds to the unperturbed system. As can be expected, this involves a more complex phase diagram, in particular a nontrivial dependence on the flatness parameter.

In this paper we consider one-dimensional systems determined by first-order differential equations with a nonlinear deterministic part and a multiplicative noise term composed of an exponentially correlated Markovian trichotomous process. For the determination of the corresponding stationary probability density an explicit second-order linear ordinary differential equation is derived. It is notable that exact formulas for the steady-state distributions can also be found for a special class of model equations that can be transformed into linear equations with additive noise terms. Comprehensive phase diagrams are presented to demonstrate the noise-induced transitions.

The structure of the paper is as follows. In Sec. II the model and exact differential equation for the stationary probability density are presented. In Sec. III a linear system with additive trichotomous noise is considered. The exact steady-state distribution is found. In Sec. IV the pure correlation-time-induced transitions and the most general properties of the stationary probability density in the phase space of the noise parameters are analyzed and the phase diagram is presented. In Sec. V the symmetric Hongler model [2,8,12] is

*Electronic address: ain@tpu.ee

taken under closer consideration. The dependence of the noise-induced transitions on the noise amplitude is investigated. The results obtained for trichotomous noises are compared with those of the dichotomous noises and the GCN models. Section VI contains a comparison of the results obtained for the Hongler model with those of the Gompertz and the generalized Verhulst models, and concluding remarks.

II. TRICHOTOMOUS MARKOVIAN NOISE

Here we explicate the idea of dichotomous noise further to a symmetric three-level random telegraph process $f(t)$ that may be called a trichotomous process. This is a random stationary Markovian process that consists of jumps between three values $a=a_0$, 0, and $-a_0$. The jumps follow in time according to a Poisson process, while the values occur with the stationary probabilities

$$P_s(a_0)=P_s(-a_0)=q, \quad P_s(0)=1-2q. \tag{1}$$

After [10] the transition probabilities between the states $f(t)=\pm a_0$ and 0 can be obtained as follows:

$$P(\pm a_0,t+\tau|0,t)=P(-a_0,t+\tau|a_0,t)=P(a_0,t+\tau|-a_0,t)$$
$$=q(1-e^{-\nu\tau}),$$
$$P(0,t+\tau|\pm a_0,t)=(1-2q)(1-e^{-\nu\tau}),$$
$$\tau>0, \quad 0<q<1/2, \quad \nu>0. \tag{2}$$

The process is completely determined by Eqs. (1) and (2). One can also calculate the mean value $\langle f\rangle$ and the correlation function $\langle f(t),f(t')\rangle$:

$$\langle f(t)\rangle=0,$$
$$\langle f(t),f(t')\rangle=\langle a^2\rangle e^{-\nu|t-t'|}=2qa_0^2e^{-\nu|t-t'|}. \tag{3}$$

It can be seen that ν is the reciprocal of the noise correlation time:

$$\nu=1/\tau_{cor}.$$

The noise intensity σ^2 is defined as

$$\sigma^2:=2\int_0^\infty \langle f(t+\tau),f(t)\rangle d\tau=4qa_0^2/\nu. \tag{4}$$

The flatness parameter δ can be expressed in a very simple way by the probability q: $\delta:=\langle f^4(t)\rangle/\langle f^2(t)\rangle^2=1/(2q)$.

Next systems described by only one variable are considered; i.e., our phenomenological kinetic equation is of the type

$$\frac{dx}{dt}=h(x)+g(x,f(t)), \tag{5}$$

where h and g are deterministic functions and $f(t)$ is a trichotomous noise. If $g(x,f(t))$ is an odd function in f, i.e., $g(x,0)=0$, then $g(x,f(t))=g(x,a_0)f(t)/a_0$ and Eq. (5) is reducible to a stochastic differential equation (SDE)

$$\frac{dx}{dt}=h(x)+g(x)f(t), \quad g(x):=\frac{1}{a_0}g(x,a_0). \tag{6}$$

For the calculation of the stationary probability density $P(x)$ the results of [13] can be applied. Notably, it is shown there that if a process $x(t)$ satisfies the stochastic differential equation (6), where $f(t)$ is a generalized random telegraph process and the probability flux vanishes, the stationary probability density $P(x)$ is a solution of the operator equation

$$h(x)P(x)=-\nu g(x)\langle a\hat{L}_a^{-1}\rangle P(x). \tag{7}$$

Here the angular brackets $\langle\;\rangle$ mean averaging over the values of the random variable a and the operator $\hat{L}_a^{-1}$ is the inverse of the operator $\hat{L}_a$ defined by

$$\hat{L}_a\psi(x)=\nu\psi(x)+\frac{d}{dx}\{[h(x)+ag(x)]\psi(x)\}.$$

In our equation (6) the random variable a takes the values $a_0,-a_0$ with the probability q and the value 0 with the probability $1-2q$ and the following differential equation for the determination of the stationary probability density $P(x)$ corresponding to Eq. (6) can be obtained from Eq. (7):

$$\nu A(x)P(x)+\frac{d}{dx}\{g(x)[A^2(x)-a_0^2]P(x)\}$$
$$=-\frac{d}{dx}\left\{A(x)B(x)\left[\nu A(x)P(x)+\frac{d}{dx}\{g(x)[A^2(x)-a_0^2]P(x)\}\right]\right\}$$
$$+(2q-1)\nu a_0^2\frac{d}{dx}[B(x)P(x)], \tag{8}$$

where

$$A:=\frac{h(x)}{g(x)}, \quad B(x):=\left[\frac{\nu}{g(x)}+\frac{d}{dx}A(x)\right]^{-1}.$$

In the case of $q=1/2$ (a dichotomous noise) the last term vanishes and Eq. (8) is satisfied by every solution of the equation

$$\nu A(x)P(x)+\frac{d}{dx}\{g(x)[A^2(x)-a_0^2]P(x)\}=0.$$

The latter corresponds to Eq. (6) in case $f(t)$ is a dichotomous noise. This has been investigated in detail by several authors [2,5,6].

In the trichotomous δ-correlated limit, $\nu\to\infty$, $a_0\to\infty$, $\sigma^2=4qa_0^2/\nu$ is finite, Eq. (8) reduces to the following Fokker-Planck equation with zero-flux boundary conditions:

$$-A(x)P(x)+\frac{\sigma^2}{2}\frac{d}{dx}[g(x)P(x)]=0.$$

Hence, the resulting steady-state distribution is

$$P(x)=\frac{c}{g}\exp\left(\frac{2}{\sigma^2}\int^x\frac{h(x)}{g^2(x)}dx\right), \tag{9}$$

where c is a normalization constant. It can be seen that the steady states for trichotomous and Gaussian δ-correlated fluctuations are indistinguishable.

It is remarkable that in the case of trichotomous noise the steady-state distribution $P(x)$ corresponding to Eq. (6) is determined by a relatively simple second-order linear ordinary differential equation and the behavior of $P(x)$ can be investigated by the general theory of such equations. Unfortunately exact solutions of Eq. (8) can be obtained but in few cases. In the next section a class of SDE's reducible to linear equations that can be handled analytically is considered in detail.

III. LINEAR SYSTEM WITH ADDITIVE TRICHOTOMOUS FLUCTUATIONS: EXACT STATIONARY PROBABILITY DENSITY

In the case of

$$g(x)\frac{d}{dx}h(x)=-rg(x)+h(x)\frac{d}{dx}g(x), \tag{10}$$

the nonlinear SDE (6) can be transformed into the linear SDE

$$\frac{dy}{dt}=-ry+f(t), \tag{11}$$

where $r>0$ is a constant, by defining a new variable

$$y=\int^{x}\frac{dx}{g(x)}+C,$$

where C is a constant. Defining $\tilde{P}(y)$ as the stationary probability density for the process $y(t)$, one can get

$$P(x)=\tilde{P}(y(x))/g(x). \tag{12}$$

In the following we restrict ourselves to systems where the condition (10) holds. One of these is the Hongler model.

The stochastic Hongler model in its dimensionless form is given by the differential equation [3,12]

$$\frac{dx}{dt}=-\frac{1}{2\sqrt{2}}\tanh(2\sqrt{2}x)+\frac{\lambda}{4\cosh(2\sqrt{2}x)},$$
$$\lambda=\lambda_0+f(t),\quad \lambda_0\geqslant 0, \tag{13}$$

where time t is measured in units of the relaxation time of the deterministic system. The Hongler model as such does not correspond to any known process in nature. But in the case of $x\ll 1$ it coincides (to the precision of members proportional to x^2) with the genetic model [2,7,14]

$$\frac{du}{dt}=1/2-u+\lambda u(1-u),\quad u=x+1/2.$$

The latter has many essential applications in genetics and chemistry. In this model

$$y=\sqrt{2}\sinh(2\sqrt{2}x)-\lambda_0,\quad r=1. \tag{14}$$

Another example is the Gompertz model [15]

$$\frac{dx}{dt}=-rx\ln\left(\frac{x}{N}\right),\quad \ln N=\ln N_0+f(t),\quad N_0>0,\quad r>0. \tag{15}$$

This equation in its deterministic form was first proposed (with $r<0$) in connection with a mortality analysis of elderly people. The appropriate transformed variable is given by

$$y=\frac{1}{r}\ln\frac{x}{N_0}. \tag{16}$$

Finally, the condition (10) is also valid to the generalized Verhulst model [15,16]

$$\frac{dx}{dt}=\frac{r}{\mu}x\left[1-\left(\frac{x}{K}\right)^{\mu}\right],\quad \mu>0,\ r>0, \tag{17}$$

in the case where the carrying capacity K fluctuates as

$$\frac{r}{\mu}\left(\frac{1}{K}\right)^{\mu}=\frac{r}{\mu}\left(\frac{1}{K_0}\right)^{\mu}+f(t),\quad K_0>0.$$

The appropriate new variable is

$$y=\frac{1}{\mu}(1/K_0^{\mu}-1/x^{\mu}).$$

Obviously, the model (17) is biologically meaningful only if

$$a_0<r/\mu K_0^{\mu}. \tag{18}$$

For the process $y(t)$ of Eq. (11) the stationary probability density $\tilde{P}(y)$ can be found. Following from the form of the process $f(t)$, the support of the stationary probability density $\tilde{P}(y)$ lies in the interval $(a_0/r,-a_0/r)$. It also follows from Eq. (11) that in the stationary state the mean value of the process y is zero, $\langle y\rangle_s=0$, and the dispersion equals

$$\langle y^2\rangle_s=\frac{2qa_0^2}{r(\nu+r)}. \tag{19}$$

It should be noted that all odd moments $\langle y^{2k+1}\rangle_s$ vanish in the stationary state and the probability density $\tilde{P}(y)$ is symmetric with respect to $y=0$. Evidently, from Eq. (8) the following second-order differential equation can be obtained for $\tilde{P}(y)$:

$$\left(\frac{\nu}{r}-1\right)\left(\frac{\nu}{r}y\tilde{P}-\frac{d}{dy}\left\{\left[y^2-\left(\frac{a_0}{r}\right)^2\right]\tilde{P}\right\}\right)$$
$$=\frac{d}{dy}\left[y\left(\frac{\nu}{r}y\tilde{P}-\frac{d}{dy}\left\{\left[y^2-\left(\frac{a_0}{r}\right)^2\right]\tilde{P}\right\}\right)\right]$$
$$+\frac{(1-2q)\nu a_0^2}{r^3}\frac{d}{dy}\tilde{P}. \tag{20}$$

By the following exchange of variables,

$$z=(ry/a_0)^2, \tag{21}$$

Eq. (20) can be transformed into a hypergeometric equation

$$z(1-z)\frac{d^2}{dz^2}W(z)+[\gamma^*-(\alpha^*+\beta^*+1)z]\frac{d}{dz}W(z) -\alpha^*\beta^*W(z)=0, \tag{22}$$

where $\gamma^*=3/2-q\nu/r$, $\beta^*=1-\nu/2r$, $\alpha^*=3/2-\nu/2r$, and $W(z(y))=\tilde{P}(y)$.

Two constants of integration of the general solution of Eq. (22) can be specified, by keeping in mind that the solution $\tilde{P}(y)=W(z(y))$ is symmetric with respect to the point $y=0$ and by the application of the normalization condition of $\tilde{P}(y)$ and of the condition (19). After quite simple but voluminous calculations it can be obtained that

$$\tilde{P}(y)=W(z)=\frac{r2^{1-\nu/r}}{a_0B(q\nu/r,(1-q)\nu/r)} \times|1-z|^{(1-q)\nu/r-1}F(\alpha,\beta;\gamma;1-z), \tag{23}$$

where $B(\lambda,\kappa)\equiv\Gamma(\lambda)\Gamma(\kappa)/\Gamma(\lambda+\kappa)$ is the beta function, F is the hypergeometric function (also known as ${}_2F_1$), Γ is the gamma function, and $\beta=\alpha-1/2=(1-2q)\nu/2r$, and $\gamma=(1-q)\nu/r$. At the values of the parameters satisfying the inequality

$$\frac{\nu}{r}>\frac{1}{2q}, \tag{24}$$

the hypergeometric series in Eq. (23) converges also at $z=0$ and consequently the form (23) can be applied to analyze the properties of the solution $\tilde{P}(y)$ in the domain of Eq. (24). In the case of

$$\frac{\nu}{r}<\frac{1}{2q}, \tag{25}$$

it is practicable, by applying the properties of the hypergeometric function, to convert Eq. (23) to the form

$$\tilde{P}(y)=W(z)=\frac{r2^{1-\nu/r}}{a_0B(q\nu/r,(1-q)\nu/r)} \times|1-z|^{(1-q)\nu/r-1}z^{q\nu/r-1/2} \times F(\gamma-\alpha,\gamma-\beta;\gamma;1-z). \tag{26}$$

The hypergeometric series in this equation converges at $z=0$, if the condition (25) is fulfilled.

IV. PURE CORRELATION-TIME-INDUCED TRANSITIONS

Next, we shall consider the most general properties of the probability density $\tilde{P}(y)$ in the phase space of the parameters q, ν, and a_0. First, it should be noted that the noise amplitude a_0 appears in $\tilde{P}(y)$ only as a scale factor. Consequently, paying no tribute to generality, one can take $a_0=1$ and $r=1$ (time is in units of macroscopic relaxation time $1/r$) when investigating the behavior of $\tilde{P}(y)$. Proceeding from Eqs. (23) and (26) one can distinguish between eight domains in the two-dimensional phase space (q,ν) (see Fig. 1).

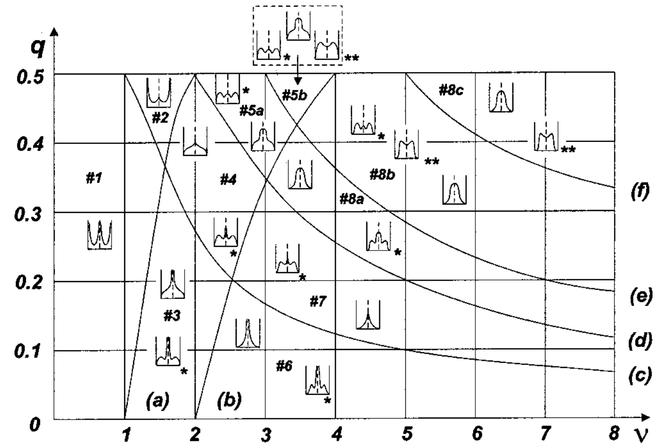

FIG. 1. The (q,ν,a_0) phase diagram for the steady-state behavior of the Hongler's model with trichotomous noise. The curves (a)–(f) correspond to the following conditions: (a) $\nu=1/(1-q)$, (b) $\nu=2/(1-q)$, (c) $\nu=1/(2q)$, (d) $\nu=1/q$, (e) $\nu=3/(2q)$, and (f) $q=3(\nu^2-4\nu+5/2)/\nu(\nu^2-3\nu-1)$. The distributions of $P(x(y))$ versus y for the different domains formed by the curves are sketched. Within the domains the effect of noise amplitude a_0 on the shape of P is denoted by asterisks: * for $a_0>\tilde{a}_{cr}$ and ** for $a_0>a_{cr}$.

No. 1: $\nu<1/(2q)$, $\nu<1/(1-q)$. In this domain the highly probable states are concentrated in the vicinity of the points $y=-1,0,1$. There the probability density approaches infinity.

No. 2: $\nu<1/(1-q)$, $\nu>1/(2q)$. Here again the most probable states are concentrated around the points $y=-1,0,1$. At the points $y=-1,1$ the probability density approaches infinity. At $y=0$ we find a local finite peak, with the derivative approaching $+\infty$, if $y\to-0$, and $-\infty$, if $y\to+0$, respectively.

No. 3: $1/(1-q)<\nu<2/(1-q)$, $\nu<1/(2q)$. The states of high probability are concentrated in the vicinity of $y=0$ where $\tilde{P}(y)\to\infty$. At the boundaries $\tilde{P}(\pm1)=0$, but there the derivative of the probability density is unbounded.

No. 4: $1/(1-q)<\nu<2/(1-q)$, $1/q>\nu>1/(2q)$. $\tilde{P}(y)$ has one finite peak, situated at $y=0$. At the boundaries the probability density is zero and at each of the three points $(y=0,\pm1)$ its derivative is unbounded.

No. 5: $1/(1-q)<\nu<2/(1-q)$, $\nu>1/q$. The probability density has the only maximum, at $y=0$, where its derivative is zero. At the boundaries $\tilde{P}(\pm1)=0$ and the derivative is unbounded.

No. 6: $\nu>2/(1-q)$, $\nu<1/(2q)$. The most probable states are near $y=0$ where $\tilde{P}(y)$ is unbounded. At the boundaries both the probability density and its derivative vanish.

No. 7: $\nu>2/(1-q)$, $1/q>\nu>1/(2q)$. The stationary probability density is monomodal with a finite peak at $y=0$. The derivative is unbounded there. At the boundaries both $\tilde{P}(\pm1)$ and its derivative vanish.

No. 8: $\nu>2/(1-q)$, $\nu>1/q$. The only most probable state is at $y=0$, where the probability density is finite and its derivative vanishes. At the boundaries both the probability density and its derivative approach zero.

All the singularities are integrable. Attention should be called to the fact that the least value of the noise correlation time $\tau_{cor}=1/\nu$ for which the three-value structure of noise is still immediately reflected in the form of the stationary probability density, depends on the probability q:

$$\tau_{cor}=1/\nu>1-q>1/2.$$

For short correlation times, i.e., in the trichotomous δ-correlated limit, it follows from Eq. (9) that $\tilde{P}(y)$ is just the Gaussian distribution function

$$\tilde{P}(y)\simeq C\exp\left(-\frac{\nu r}{4qa_0^2}y^2\right), \tag{27}$$

where C is the normalization coefficient.

Returning to the probability density (12) specific to our initial problem of the stochastic equation, it should be noted that all attributes of $\tilde{P}(y)$ by which the phase domains Nos. 1–8 were distinguished on the diagram, i.e., the singularities of $\tilde{P}(y)$ and of its derivative at the points $y=\pm 1,0$, also characterize the probability density $P(x)$.

V. NOISE-INDUCED TRANSITIONS OF THE HONGLER'S MODEL

In order to discuss the influence of a noise amplitude a_0 on the shape of the steady-state distribution $P(x)$, the symmetric ($\lambda_0=0$) Hongler model (13) is taken under closer consideration. By denoting $z\equiv y^2/a_0^2$ one can get

$$P(x)=4\sqrt{1+a_0^2z/2}\,W(z), \tag{28}$$

where $W(z(y))=\tilde{P}(y)$ and y is determined by Eq. (14). Investigating the extrema of function (28) near the point $y=0$, it is easy to conclude that the most probable state at the point $z=0$ in domains Nos. 5b, 8b, and 8c of the phase space (ν,q) [where $\nu>3/(2q)$] may disappear as the noise amplitude exceeds a critical value a_{cr}. Instead of a local maximum of $P(x)$ there will be a minimum at $y=0$, symmetrically to which new local maxima are formed at both sides. The latter move away from $y=0$ as a_0 continues growing. The critical noise amplitude is given by

$$a_{cr}^2=\frac{2(\nu-2)(\nu-3)}{2q\nu-3}. \tag{29}$$

It can be easily seen that a_{cr}^2 has a minimum at the value of the correlation time $\tau\equiv 1/\nu$:

$$\tau_1=(5-4q)^{-1}[1-\sqrt{(1/3)(3-4q)(1-2q)}]\leqslant 1/3. \tag{30}$$

The minimal value of the critical parameter $a_{cr}^2(\tau_1)=2(1/\tau_1^2-6)\geqslant 6$ monotonously decreases as τ_1 increases. It is interesting to note that in domains Nos. 5a and 8a $[1/q<\nu<3/(2q)]$, where the probability density $P(x)$ also has a smooth maximum (the derivative is zero) at $y=0$, there is no such local phase transition; i.e., there is no critical amplitude a_{cr} at which the peak-damping mechanism is replaced by a peak-splitting one.

As a_0 is growing, phase transitions different from those considered can be observed in domains Nos. 3–8 of the phase space $[\nu>1/(1-q)]$. Notably, if a_0^2 exceeds a critical value $\tilde{a}_{cr}^2$ (in general, $\tilde{a}_{cr}^2\neq a_{cr}^2$), then the probability density $P(x)$ can be characterized by three probability maxima on the graph. This characteristic causes domain No. 8c in the phase diagram in Fig. 1, separated from domain No. 8b by the curve (f) determined by

$$q=\frac{3(\nu^2-4\nu+5/2)}{\nu(\nu^2-3\nu-1)},\quad \nu\geqslant 5. \tag{31}$$

On the left side of this curve, $\tilde{a}_{cr}^2<a_{cr}^2$, and as the noise amplitude grows, there will be two phase transitions: at the increasing of a_0^2 over $\tilde{a}_{cr}^2$ there is a transition from a phase with one probability density maximum to one with three maxima, while at a further increase over $a_0^2=a_{cr}^2$ there is a transition to a phase with two maxima. At the right side of the curve (31) a phase transition occurs between phases with one and two maxima.

In the case of dichotomous noise $q=1/2$ and so we have $\tilde{a}_{cr}^2=a_{cr}^2=2(\nu-2)$. As to the interval $2<\nu<3$ belonging to domain No. 5a, where trichotomous noise generates either one or three maxima to the probability density, the limit of $q\to 1/2$ leads to the disappearance of the central maximum.

As the calculation of the critical parameter $\tilde{a}_{cr}^2$ in the general case requires the solution of a transcendental equation, it is impossible to determine $\tilde{a}_{cr}^2$ by simple expressions like Eq. (29). Actually, numerical values can be obtained by computer and some estimations can also be made. Still, a precise analysis is possible at those points of the phase space where the probability density $P(x)$ is expressed by elementary functions. This could be illustrated by the following examples.

(i) On the curve $\nu=1/q$ (see Fig. 1) the density $P(x)$ takes the form

$$P(x)=\frac{2(\nu-1)}{a_0}\sqrt{1+\frac{y^2}{2}}\left(1-\frac{|y|}{a_0}\right)^{\nu-2}.$$

It can be seen easily that the critical parameter $\tilde{a}_{cr}^2$ is given by

$$\tilde{a}_{cr}^2=8(\nu-2)(\nu-1).$$

(ii) For the point $\nu=6,\quad q=1/3$ (domain No. 8b) one can get

$$P(x)=C\sqrt{1+\frac{y^2}{2}}\left(1-\frac{|y|}{a_0}\right)^3\left(\frac{|y|}{a_0}+\frac{1}{3}\right),$$

where C is the normalizing coefficient. Three phases with the transitions at $\tilde{a}_{cr}^2=22.5$ and $a_{cr}^2=24$ can be discerned.

(iii) In the point $\nu=2,\quad q=1/4$ [see curve (c) in Fig. 1] the probability density $P(x)$ takes the form

$$P(x)=\frac{1}{2\pi a_0}\sqrt{1+\frac{y^2}{2}}\ln\left|\frac{1+\sqrt{1-y^2/a_0^2}}{1-\sqrt{1-y^2/a_0^2}}\right|.$$

The critical parameter equals $\tilde{a}^2_{cr} \approx 27.09$.

The phase diagram of the Hongler model with trichotomous noise displayed in Fig. 1 is rather complicated, consisting of 16 different phases. Analogously, dichotomous noise induces five phases in the phase space (a_0, ν), whereas Gaussian colored noise does but two [2]. However, there is a common feature for the phase transitions of these three noise patterns at the Hongler model: a growth of the noise intensity changes the central maximum of the probability density at $y=0$ to a minimum; i.e., the maximum is split into two (see Fig. 1, domains Nos. 5b, 8b, and 8c). Following [2], one can see that in the cases of both the Hongler model with trichotomous as well as dichotomous noises and the GCN model, the noise correlation time τ_{cor} influences the location of the pure noise-induced transition point at which the stationary distribution at $y=0$ switches over from a monomodal to a bimodal behavior. Recall that in the white noise case the critical variance at which this phenomenon occurs is $\sigma^2 \equiv \sigma_c^2 = 4$. In the case of GCN with the correlation function

$$\langle f(t+\tau), f(t) \rangle = \frac{\mu^2}{2\nu} e^{-\nu|\tau|}, \quad \nu \equiv 1/\tau_{cor},$$

the white-noise limit corresponds to $\mu \to \infty$, $\nu \to \infty$ such that $\mu^2/\nu^2 = \sigma^2$ is finite. Hence, for white noise one can write

$$\sigma_c^2 = \left(\frac{\mu}{\nu}\right)_c^2 = 4,$$

which could be compared with the corresponding value for the GCN case:

$$\sigma_c^2 = \left(\frac{\mu}{\nu}\right)_c^2 = 4 + 4\tau_{cor}.$$

Here the effect of the nonvanishing noise correlation time increases the noise intensity, which is necessary to induce transitions [2]. In the case of dichotomous noise the white-noise limit corresponds to $a_0 \to \infty$, $\nu \to \infty$ such that $\sigma^2 = 2a_0^2/\nu$ is finite. The intensity σ_c^2, necessary to induce critical behavior in the model, decreases as the correlation time $\tau_{cor} = 1/\nu$ increases [2]:

$$\sigma_c^2 = \left(\frac{2a_0^2}{\nu}\right)_c = 4 - 8\tau_{cor}, \quad \tau_{cor} < 1/2.$$

There is an upper limit for the noise correlation time, beyond which the critical behavior disappears.

In the case of trichotomous noise the white-noise limit corresponds to $a_0 \to \infty$, $\nu \to \infty$ such that $\sigma^2 = 4qa_0^2/\nu$ is finite. The intensity σ_c^2, necessary to induce critical behavior in the model, is of the form

$$\sigma_c^2 = \left(\frac{4qa_0^2}{\nu}\right)_c = 4(1-2\tau_{cor}) \times \left(1 + 3\tau_{cor}\frac{1-2q}{2q-3\tau_{cor}}\right) > 4 - 8\tau_{cor},$$

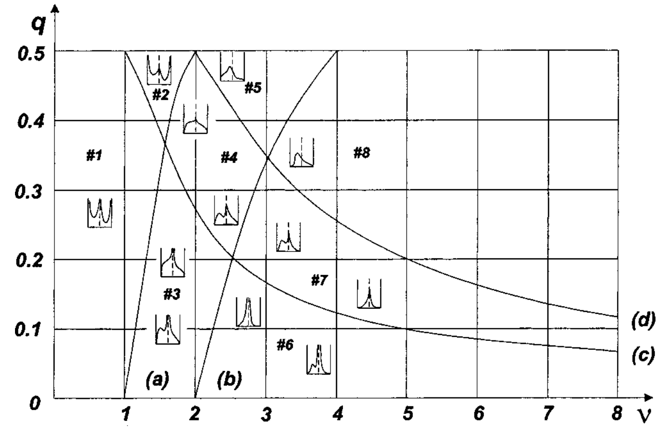

FIG. 2. The (q, ν, a_0) phase diagram for the steady-state behavior of the Gompertz' and generalized Verhulst models with trichotomous noise. The curves (a)–(d) coincide with those in Fig. 1: (a) $\nu = 1/(1-q)$, (b) $\nu = 2/(1-q)$, (c) $\nu = 1/(2q)$, and (d) $\nu = 1/q$. The distributions of $P(x(y))$ versus y for the different domains formed by the curves are sketched. In domains Nos. 3, 4, 6, and 7 the variants with additional extrema are caused by the condition $a_0 > \tilde{a}_{cr}$.

$$\tau_{cor} < 2q/3. \tag{32}$$

There is also an upper limit for the noise correlation time, beyond which the critical behavior disappears. Evidently, σ_c^2 tends to infinity, if $\tau_{cor} \to 2q/3$ and $q \neq 1/2$. It can also be seen that if $q < 0.3$, then the critical intensity of the noise σ_c^2 increases monotonously as τ_{cor} increases. In this sense the model resembles the GCN Hongler model.

In case $q > 0.3$ there is another critical value for the correlation time:

$$\tau_2 = \frac{1}{3}[2q - \sqrt{(3-4q)(1/2-q)}].$$

If the correlation time is less than that, $\tau_{cor} < \tau_2$, then as τ_{cor} decreases, σ_c^2 increases and vice versa. Thus, one can see here common features with models with dichotomous noises.

It is most remarkable that there is not only an upper limit for the noise correlation time, present also in the case of dichotomous noises, but there appear also nonzero minima of the critical intensity $\sigma_c^2(\tau_{cor})$ at $\tau_{cor} = \tau_2, q > 0.3$:

$$\sigma_c^2(\tau_2) = 4(1 - 6\tau_2^2) \geq 4/3.$$

VI. DISCUSSION

We have applied the method used in Secs. IV and V to the Gompertz and generalized Verhulst models, Eqs. (15) and (17). Their phase diagrams are similar to each other, while 12 different phases can be distinguished there (see Fig. 2). Compared with the symmetric Hongler model there are the following characteristic features beside asymmetry: (i) There are no extrema of the stationary probability density at the values $y > 0$ in the domain of $\nu > 1/(1-q)$ (domains Nos. 3–8). (ii) In domains Nos. 5 and 8 (where $\nu > 1/q$) $P(x(y))$ is monomodal at any value of the noise amplitude a_0; at a growing a_0 the maximum shifts to lesser values of y. (iii)

The asymmetric Hongler model (where $\lambda_0 < 0$) at a decreasing λ_0 behaves ever more similarly to the Gompertz and Verhulst models, especially if $a_0 < |\lambda_0|$.

A major virtue of the models with trichotomous noise is that they constitute another case admitting an exact analytical solution for the stationary probability density for any value of the correlation time and the flatness parameter $\delta = 1/(2q)$. Though both the dichotomous and trichotomous noises may be too rough approximations in most practical cases, the latter is more flexible, including all cases of the dichotomous noises and, as such, revealing the essence of the peculiarities of the latter.

It is worth while mentioning that experimental evidence of noise-induced transitions has been obtained (for reference surveys see [2,3]). Markovian trichotomous noise is rather well suited for experimental realization and hence a detailed quantitative comparison of experimental results and theoretical predictions should be feasible. We envisage direct applicability of models with trichotomous noises in some bio- and ecosystems. For instance, wind either can carry the seeds of a plant to different directions (two in a one-dimensional case) depending on its direction (noise parameter $a = \pm a_0$) or nowhere ($a = 0$) if its speed does not exceed a critical value. The same way casual water flow in a lake either can or cannot cause a flux of sediments and, in principle, the phases met in our diagrams may well emerge in some way in the resulting sediment distributions. In natural systems transport of particles can also be caused by noise-induced currents generated at ratchetlike potentials. As has been shown [10], the value of the noise flatness can be decisive for both the intensity and the direction of the current, and besides it can cause a separation of particles. It is remarkable that with the trichotomous noises the flatness parameter, contrary to the dichotomous and GCN noises, can be anything from 1 to ∞.

Details known about the solutions of Eq. (8) may be of use in testing approximate methods in the theory of stochastic differential equations.

[1] P. Jung, Phys. Rep. **234**, 175 (1993).

[2] W. Horsthemke and R. Lefever, *Noise-Induced Transitions* (Springer-Verlag, Berlin, 1984).

[3] K. Lindenberg and B. West, *The Nonequilibrium Statistical Mechanics of Open and Closed Systems* (VCH, New York, 1990).

[4] M. I. Dykman, R. Mannella, P. V. E. McClintock, N. D. Stein, and N. G. Stocks, Phys. Rev. E **47**, 3996 (1993).

[5] K. Kitahara, W. Horsthemke, and R. Lefever, Phys. Lett. **70A**, 377 (1979).

[6] K. Kitahara, W. Horsthemke, R. Lefever, and Y. Inaba, Prog. Theor. Phys. **64**, 1233 (1980).

[7] H. Matsuda and K. Ishii, J. Math. Biol. **11**, 119 (1981).

[8] R. Mankin, A. Ainsaar, and A. Haljas, Proc. Estonian Acad. Sci. Phys. Math. (to be published).

[9] M. Bier, Phys. Lett. A **211**, 12 (1996).

[10] C. Berghaus, U. Kahlert, and J. Schnakenberg, Phys. Lett. A **224**, 243 (1997).

[11] C. R. Doering, W. Horsthemke, and J. Riordan, Phys. Rev. Lett. **72**, 2984 (1994).

[12] M. O. Hongler, Helv. Phys. Acta **52**, 280 (1979).

[13] V. I. Klyatskin, *Stohasticheskie Uravneniya i Volny v Sluchaino-Neodnorodnyh Sredah* (Nauka, Moskva, 1980).

[14] L. Arnold, W. Horsthemke, and R. Lefever, Z. Phys. B **29**, 367 (1978).

[15] N. S. Goel and N. Richter-Dyn, *Stochastic Models in Biology* (Academic Press, London, 1974).

[16] R. Levins, Proc. Natl. Acad. Sci. USA **62**, 1061 (1969).